Technical Note

DNA single-base mismatch study using graphene oxide nanosheets based fluorometric biosensor

Yinxi Huang, Hui Ying Yang, and Ye Ai

Anal. Chem., **Just Accepted Manuscript** • DOI: 10.1021/acs.analchem.5b03037 • Publication Date (Web): 24 Aug 2015

DNA single-base mismatch study using graphene oxide nanosheets based fluorometric biosensor

Yinxi Huang, Hui Ying Yang, and Ye Ai*

Pillar of Engineering Product Development, Singapore University of Technology and Design, Singapore 487372, Singapore

* Corresponding author. Email: aiye@sutd.edu.sg; Tel: (+65) 6499 4553

Abstract

Single nucleotide polymorphisms (SNPs) are frequently associated with various gene-related human diseases, whose determination has attracted great interest. Herein we report a graphene oxide (GO) nanosheets based fluorometric DNA biosensor to study the type and location of the single-base mismatch, as well as the influence of the strands length. The results indicated that both short and long targets led to much lower fluorescence signals than the perfectly complementary target, while the mismatched base type had negligible influence on the results. Furthermore, targets with mismatch location near the 5' end led to higher fluorescence intensity than those near the 3' end when the dye was tagged at the 5' end of probe.

Introduction

The development of novel, ultrasensitive DNA biosensors has gained extensive interest for applications in different areas such as food industry, environment, pharmaceutics, disease diagnosis, and so on. As the presence of base mutation is frequently associated with gene-related human diseases, detecting a single-base mismatch is of great importance.[1,2] Various techniques for genotyping single nucleotide polymorphisms (SNPs), which is the single-base variation in a given and defined genetic location, have been reported in recent years, including DNA sequencing[3] and other DNA biosensing methods such as surface plasmon resonance,[4,5] electrochemical detection,[6,7] quartz crystal microbalance,[8,9] surface acoustic wave[10] and so on. However, all these techniques have their specific advantages and disadvantages.[3,11] For example, classic methods such as DNA sequencing exhibit high specificity and can detect unknown SNPs, but limited by the complex procedure and lengthy operation time. The throughput of biosensing techniques cannot achieve large-scale genotyping and the sample usually requires pre-treatment. Thus, developing a sensitive, rapid, easy-to-use, and cost-effective method to identify SNPs is still a challenge.

Over the past few years, many nanomaterials including gold nanoparticles,[12,13] carbon nanotubes,[14,15] graphene oxide,[16-18] and MoS_2 [19-21] have been served as ‘‘nanoquenchers’’ in various fluorometric biosensors because of their high quenching efficiencies and good biocompatibilities. Identification of single-base mutation in DNA sequence, in other words single-base mismatch with its complementary DNA, is the basis of SNPs genotyping. For example, graphene oxide (GO) has been used to develop a highly sensitive fluorescent method for DNA detection with excellent SNP discrimination.[22] As noted, these methods generally employ short dye-labeled DNA probes (~ 20-mer), which possess low fluorescence ratios between perfectly complementary DNA and the SNP sequence. Ideally, for short probe sequences, both the fluorescence of unhybridized probes in the absence of target DNA as well as in the presence of single-base mismatched target DNA could be efficiently quenched by GO, while the hybridized double-stranded DNA (dsDNA) with complementary target DNA led to observable fluorescence. However, in practical applications of DNA detection, the target sequences are normally longer. Meanwhile, the quenching efficiency of GO for long single-stranded DNA (ssDNA) is lower than short ssDNA.[23] Hence, in this study we used a

sequence with moderate length (40-mer) as probe DNA to test SNPs, while its complementary target is part of *E.coli* O157:H7 *eae*A gene sequence. The effect of the length of the target DNA on the fluorometric biosensing has been studied. In order to develop more ultrasensitive, simple, highly selective, and cost-effective biosensors, a previously developed microfluidic channel device was integrated to obtain and process measurements from very small volumes of samples with efficiency and speed.[20] For the first time we investigated the mismatched strands with different location and type of mutation using the GO based fluorometric DNA biosensor.

Experimental Section:

Chemicals and Instrumentation

DNA oligonucleotides were synthesized and purified by Integrated DNA Technologies Pte Ltd. Other chemicals were purchased from Sigma-Aldrich Pte Ltd. The deionized water was purified using a Millipore filtration System and used in all experiments. Fluorescence images were taken on a fluoscopy (Leica MC120 HD). Fluorescence spectra were measured by Ramen spectroscopy (WITec alpha300 R). All measurements were performed in 1 x phosphate buffered saline (PBS, pH 7.4) at room temperature.

Preparation of GO nanosheets

GO nanosheets were prepared by a modified Hummer's method.[24] Briefly, graphite powder (5 g) was oxidized in a hot solution (80 °C) of concentrated H_2SO_4 (39 mL) containing $K_2S_2O_8$ (2.5 g) and P_2O_5 (2.5 g), slowly cooling to room temperature over a period of 6 h. The mixture was then diluted, filtered, rinsed, and dried for 8 h at 60 °C. These pre-oxidized graphite powder (2 g) and $NaNO_3$ (1.5 g) were added to 46mL of H_2SO_4, to which $KMnO_4$ (4 g) was gradually introduced under continuous stirring in an ice-bath. The solution was further stirred for 2 h at 35 °C, and distilled water (92 mL, 70 °C) was added. The obtained brown dispersion was centrifuged and washed for several times.

Fluorescent DNA Assays

The fluorescence measurement method was the same as our previous work.[20] A PDMS device with zigzag-shaped microchannels was designed for uniform mixing of various

samples, and Raman spectroscope was used to measure the fluorescence spectra at the end of the microchannels. The results are recorded at the excitation wavelength of 532 nm. In a typical DNA assay, the fluorescence probe P1 was hybridized with the targets in 1 x PBS (pH 7.4) for 30 min, the obtained solution was mixed with GO (0.1 mg/mL) using the microfluidic device. All the concentrations mentioned in the following measurements are final concentrations in the mixture.

Results and Discussion

As illustrated in Figure 1, a TAMRA-labeled probe DNA (P1) was used for the detection. The sequences of all DNA oligonucleotides were shown in Table 1. GO nanosheets (SEM image is shown in Figure 1 inset) could adsorb dye-labeled ssDNA (P1) *via* the van der Waals force between nucleobases and the basal plane of GO nanosheets and then quench its fluorescence. When P1 was hybridized with its perfect complementary target DNA (T1) and formed dsDNA, its fluorescence would be well maintained after addition of GO because of the weak GO/dsDNA binding. Hence the fluorescence intensity of P1 could provide a quantitative indication of T1. Similarly, due to the length of DNA (40-mer), the single-base mismatched sequence (away from the base mismatched) was able to partially hybridize with probe DNA and form a non-perfect dsDNA. Hence, single-base mismatched target for P1 could also be detected using this assay. In contrast, P1 could not form dsDNA with its non-complementary DNA (N1), resulting in quenching of its fluorescence due to the absorption on GO surface.

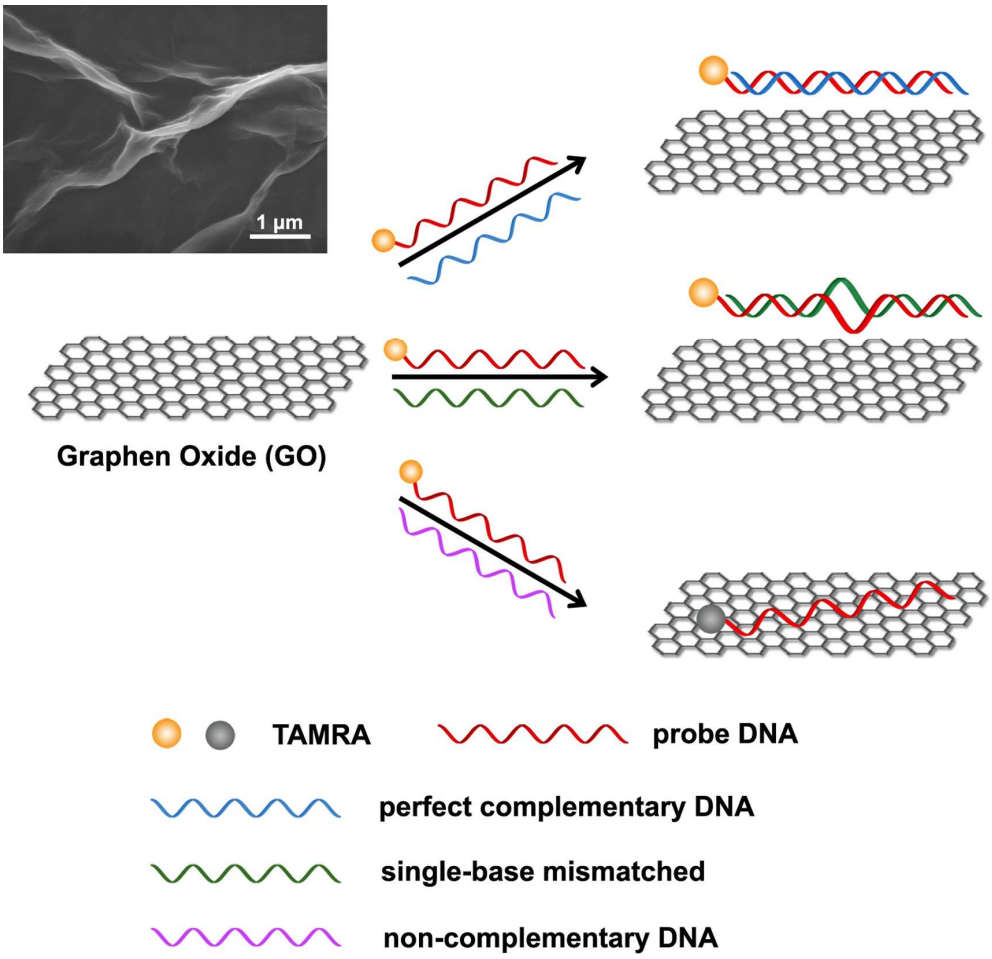

Figure 1. Schematic illustration of the GO based fluorometric DNA sensing assay. Inset: SEM image of GO nanosheets.

Table 1. DNA sequences used in this work.

DNA name	Sequence (5'-3')
P1: TAMRA-labeled probe	GGTATAAGTAATGGTATCGGCGTTATCCGCTTTAGCCGAA
T1: complementary target for P1	TTCGGCTAAAGCGGATAACGCCGATACCATTACTTATACC
T2: short target for P1	TTCGGCTAAAGCGGATAACG
T3: long target for P1	TTCGGCTAAAGCGGATAACGCCGATACCATTACTTATACCGCGACGGTG AAAAAGAATGG
M4A: 20th base mismatched target for P1	TTCGGCTAAAGCGGATAAC***A***CCGATACCATTACTTATACC
M4C: 20th base mismatched target for P1	TTCGGCTAAAGCGGATAAC***C***CCGATACCATTACTTATACC
M4T: 20th base mismatched target for P1	TTCGGCTAAAGCGGATAAC***T***CCGATACCATTACTTATACC
M1: 5th base mismatched target for P1	TTCG***T***CTAAAGCGGATAACGCCGATACCATTACTTATACC
M2: 10th base mismatched target for P1	TTCGGCTAA***C***GCGGATAACGCCGATACCATTACTTATACC

M3: 15th base mismatched target for P1	TTCGGCTAAAGCGG***C***TAACGCCGATACCATTACTTATACC
M5: 25th base mismatched target for P1	TTCGGCTAAAGCGGATAACGCCGA***C***ACCATTACTTATACC
M6: 30th base mismatched target for P1	TTCGGCTAAAGCGGATAACGCCGATACCA***C***TACTTATACC
M7: 35th base mismatched target for P1	TTCGGCTAAAGCGGATAACGCCGATACCATTACT***C***ATACC
N1: non-complementary sequence for P1	CTGCAAGACCGGATTCTGCAAGACCGGATTCTGCAAGACC

The fluorescence measurement method was the same as our previous work.[20] A PDMS device with zigzag-shaped microchannels was designed for uniform mixing of various samples. For fluorescence measurements using fluorophotometer, normally at least hundreds of μL samples are needed. By using this microfluidic device, the effective volume of DNA solution inside the microchannel is only less than 0.2 μL, which means that for the same sensing concentration, this platform can detect much less amount of DNA samples. All fluorescence signals were recorded using Raman spectroscope, and error bars are obtained from at least 6 groups of data.

Similar to previously reported studies,[17,22] when P1 was hybridized with its complementary target T1 to form a dsDNA, the fluorescence partially remained in the presence of GO, and the fluorescence was intensified along with the increase of the target concentration, with a linear range of 0 - 50nM and detection limit of 1 nM (Figure 2A). Importantly, due to the effective volume of DNA solution inside the microchannel, this microfluidic biosensor can detect as low as ~ 0.2 fmol target DNA, which is much lower than previous GO-based fluorescent methods.[17] Then we interrogated the hybridization between the probe and targets with different lengths (20-mer versus 60-mer). As shown in Figure 2B and 2C, at the same concentration, both short and long targets led to much smaller fluorescence signals than T1 that was of the same length as P1. And we also observed that the fluorescence signal for T3 (60-mer) was stronger than that of T2 (20-mer). This difference may be attributed to the length of target DNA as well as the location of dye and its interaction with GO. As shown in Figure 2D, since the length of P1 was longer than T2 and shorter than T3, they would form a mixture of ssDNA and dsDNA after hybridization. As a result, TAMRA tended to be absorbed on the surface of GO due to the presence of ss regions in both P1/T2 and P1/T3. However, as TAMRA was tagged at the 5' end of P1, it was located right at the end of ssDNA region after hybridization with T2; in contrast, it was located at the interface of the ssDNA and dsDNA regions for T3. Hence, TAMRA was more likely to be partially detached from the GO

surface in the case of P1/T3. From above tests we noted that, it was not realistic to detect long target with very short probe DNA using the fluorometric assay. As we mentioned, it is important and necessary to study longer probe performance using this method.

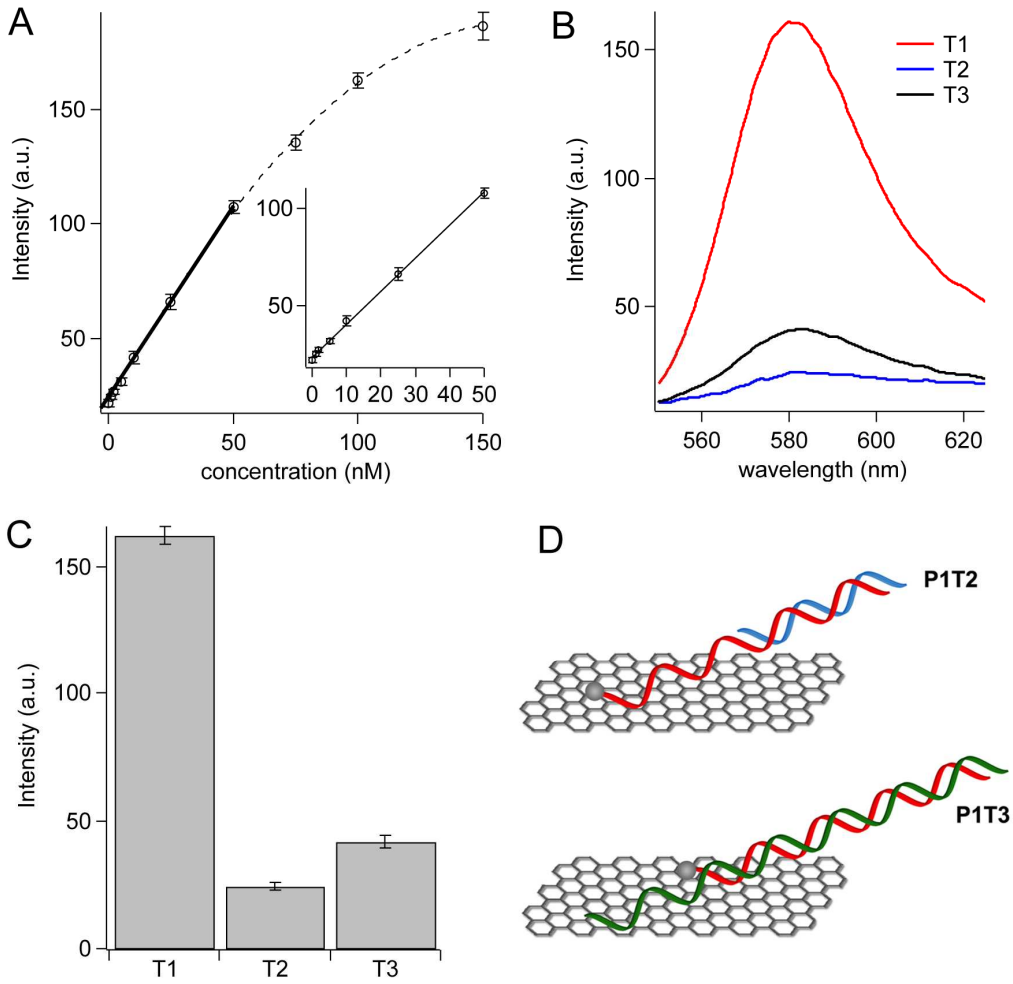

Figure 2. (A) Fluorescence intensity of P1 (100 nM) with different concentrations (0, 1, 2, 5, 10, 25, 50, 75, 100 and 150 nM) of T1 in the presence of GO. Inset: Amplification of the linear range (0–50 nM) of the calibration curve. (B) Typical fluorescence spectra and (C) Fluorescence intensity of P1 (100 nM) with different lengths of target DNA T1, T2 and T3 (100 nM) in the presence of GO. (D) Scheme for P1 in the presence of short target DNA (T2) and long target DNA (T3).

For short probe DNA, the GO-based fluorometric DNA detection exhibited high sequence specificity to easily differentiate single-base mismatches, which offered the opportunity to allow SNPs analysis. However, the results might be different for longer sequence since

single-base mismatched target could also partially hybridize with probe DNA and form a mixture of ssDNA and dsDNA. The position effect could also have an influence on the fluorescence due to the location of mismatched base and its interaction with GO. In this case, single-base substitutions were located at the 5th, 10th, 15th, 20th, 25th, 30th and 35th positions of targets (from 5' end), named as M1, M2, M3, M4, M5, M6 and M7, respectively. In order to evaluate the base type influence, we took M4 for example, where C-G bond was changed to C-A (M4A), C-C (M4C) and C-T (M4T), respectively. As shown in Figure 3, the fluorescence of P1/M4 with different mismatched base showed similar intensity in the presence of GO, indicating that base difference effect was very minor in this DNA assay, which could be ignored in the following experiments.

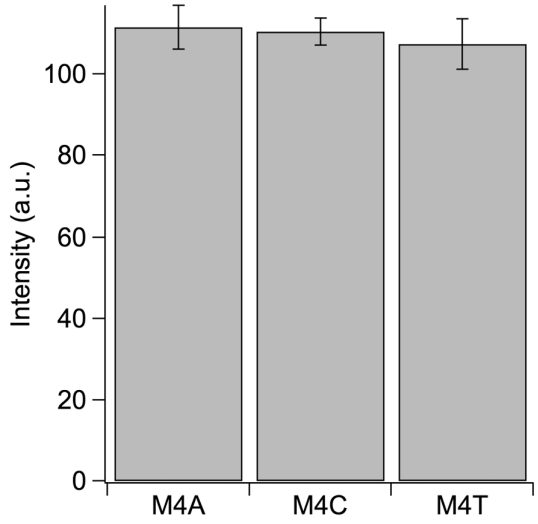

Figure 3. Fluorescence intensity of P1/M4 with different mismatched base (A, C and T) in the presence of GO.

As shown in Figure 4, the targets with different mismatch positions hybridized with P1 were detected in the presence of GO. In a typical measurement, the fluorescence signals for those single-base mismatched targets, which was of the same concentration as P1, were recorded in Figure 4A. We could observe that the signals decreased from M1 to M7 accordingly, which meant that targets with mismatch positions near the 5' end led to higher fluorescence intensity than those near the 3' end. Especially, the difference for M6 and M7 was very obvious, while those for M1 to M5 were smaller (Figure 4B). As illustrated in Figure 4C, P1

and single-base mismatched targets could form a mixture of ssDNA and dsDNA after hybridization, while regions near the mismatched base might be single-stranded. Since TAMRA was tagged at the 5' end of P1, when the mismatch position was near the 3' end of target DNA (e.g. M6, M7), the dye was located near the ss region after hybridization, more likely to be absorbed on the surface of GO, thus the fluorescence was quenched. In contrast, when the mismatch position was near the 5' end of target, TAMRA was located right at the ds region. Hence, when the ssDNA region was absorbed on the surface of GO, the dye was still far away from GO so that the fluorescence could not be fully quenched. We supposed that for M1 to M5, the signal-decreasing trend existed because that the distance from TAMRA to ss region increased. However, since the majority of the labeled dye might not be quenched by GO, the signal difference was not so great between each other. The discrimination was observed over various concentrations (Figure 4D), while the difference was hard to be discriminated for lower concentration (< 25 nM). According to the efficient sample volume inside the microchannels, the SNPs of different locations could be discriminated as low as ~5 fmol.

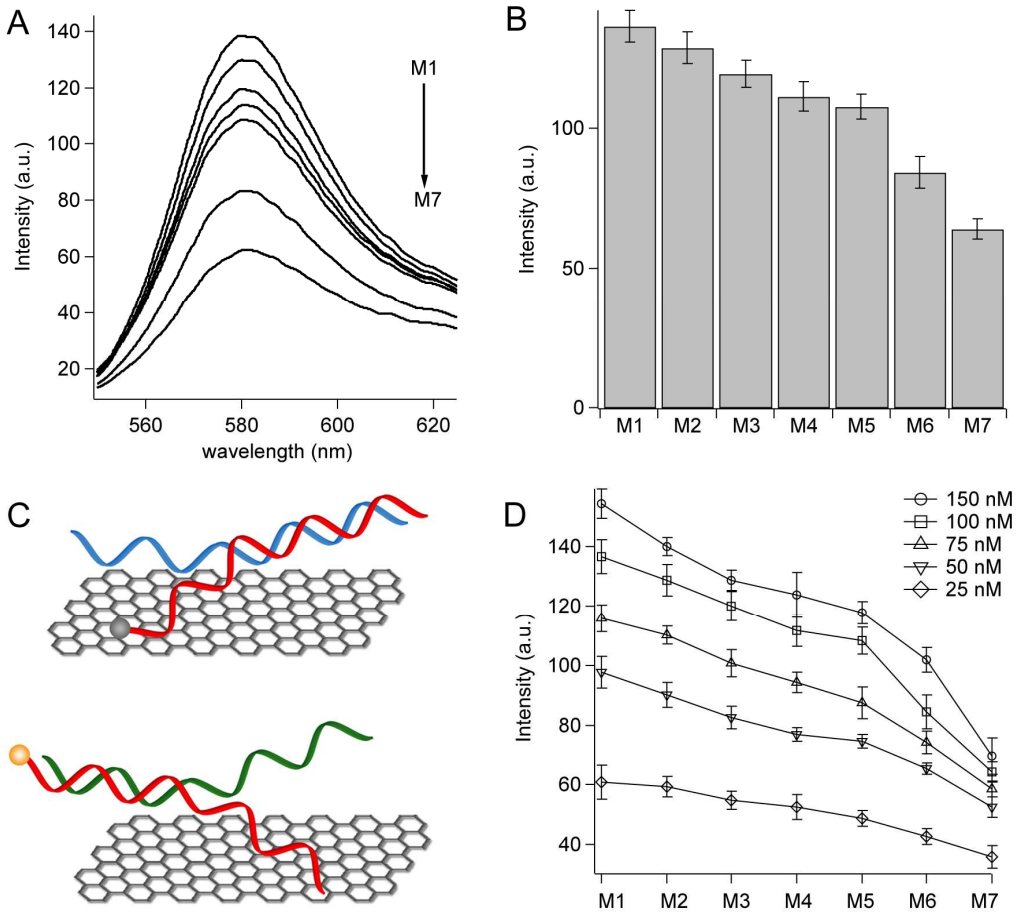

Figure 4. (A) Typical fluorescence spectra and (B) Fluorescence intensity of P1 (100 nM) with different single-base mismatched DNA M1, M2, M3, M4, M5, M6, and M7 (100 nM) in the presence of GO. (C) Scheme for DNA detection with single mismatched base of different location in the presence of GO. (D) Fluorescence intensity of P1 in the presence of different concentrations of single-base mismatched DNA (M1, M2, M3, M4, M5, M6, and M7).

We also compared the calibration curves for DNA detection of various concentrations (0, 1, 2, 5, 10, 25, 50, 75, 100 and 150 nM). As shown in Figure 5, M1, M4 and M7 were taken as typical single-base mismatched targets, which led to obvious discrimination of position effect. All the signals for single-base mismatched targets were lower than the perfectly complementary target T1, which might be due to the competition between GO/probe adsorption and probe/target hybridization, so that GO possibly competitively destabilized

mismatched duplexes. Meanwhile, random non-complementary DNA (N1) could not induce a distinct fluorescence increase, even at very high concentration.

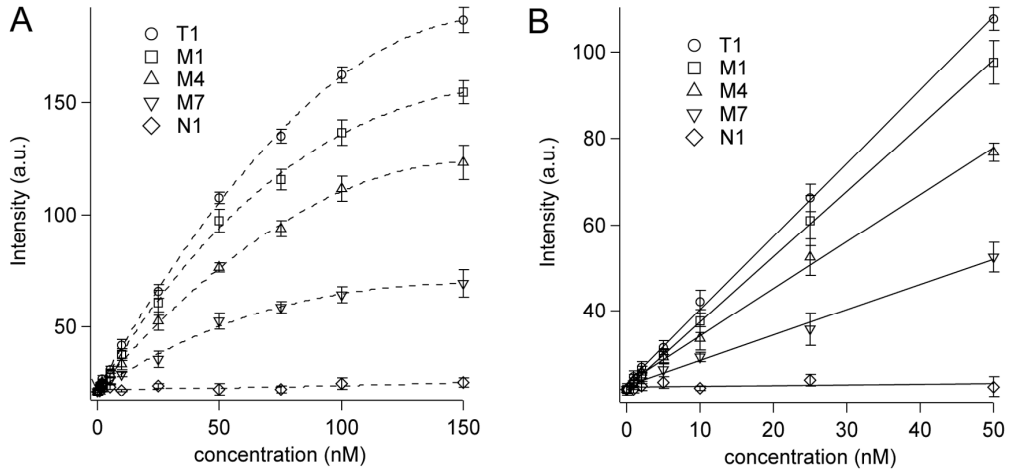

Figure 5. (A) Fluorescence intensity of P1 (100 nM) with different concentrations (0, 1, 2, 5, 10, 25, 50, 75, 100 and 150 nM) of T1, M1, M4, M7 and N1 in the presence of GO. (B) Amplification of the linear range (0–50 nM) of the calibration curve.

Conclusions

In summary, for the first time, we developed a GO based microfluidic biosensor for DNA single-base mismatch study. The type and location of the single-base mismatch, as well as the influence of the length of the strands, was investigated. By applying a 40-mer probe DNA (P1), both short (20-mer) and long (60-mer) targets led to much lower fluorescence signals than the complementary target T1 that was of the same length as P1. The mismatched base type had negligible influence on the results. Furthermore, 7 mismatched strands with different locations were studied. The results indicated that targets with mismatch location near the 5' end led to higher fluorescence intensity than those near the 3' end when the dye was tagged at the 5' end of probe. The signal difference was especially obvious for the targets with mismatched base very near the 3' end. Discrimination can be observed over a wide interval of concentrations. Although the exact mismatch location of the target DNA still cannot be determined using this assay, our studies could provide insights into improving the performance of DNA biosensors, especially for SNP genotyping.

Acknowledgements

This work was supported by the SUTD-MIT International Design Center (IDG11300101) and the TL@SUTD Seed Grant (IGDS S14 02011) awarded to Y. A.

References

(1) McCarthy, J. J.; Hilfiker, R. *Nat. Biotechnol.* **2000**, *18*, 505-508.

(2) Stoneking, M. *Nature* **2001**, *409*, 821-822.

(3) Syvanen, A. C. *Nat. Rev. Genet.* **2001**, *2*, 930-942.

(4) Li, Y. A.; Wark, A. W.; Lee, H. J.; Corn, R. M. *Anal. Chem.* **2006**, *78*, 3158-3164.

(5) Okumura, S.; Kuroda, R.; Inouye, K. *Appl. Biochem. Biotechnol.* **2014**, *174*, 494-505.

(6) Liu, G.; Lin, Y. *J. Am. Chem. Soc.* **2007**, *129*, 10394-10401.

(7) Yang, A. H. J.; Hsieh, K.; Patterson, A. S.; Ferguson, B. S.; Eisenstein, M.; Plaxco, K. W.; Soh, H. T. *Angew. Chem. Int. Ed.* **2014**, *53*, 3163-3167.

(8) Wang, D.; Tang, W.; Wu, X.; Wang, X.; Chen, G.; Chen, Q.; Li, N.; Liu, F. *Anal. Chem.* **2012**, *84*, 7008-7014.

(9) Zhang, Y.; Lin, F.; Zhang, Y.; Li, H.; Zeng, Y.; Tang, H.; Yao, S. *Anal. Sci.* **2011**, *27*, 1229-1235.

(10) Xu, Q.; Chang, K.; Lu, W.; Chen, W.; Ding, Y.; Jia, S.; Zhang, K.; Li, F.; Shi, J.; Cao, L.; Deng, S.; Chen, M. *Biosens. Bioelectron.* **2012**, *33*, 274-278.

(11) Chang, K.; Deng, S.; Chen, M. *Biosens. Bioelectron.* **2015**, *66*, 297-307.

(12) Song, S.; Liang, Z.; Zhang, J.; Wang, L.; Li, G.; Fan, C. *Angew. Chem. Int. Ed.* **2009**, *48*, 8670-8674.

(13) Lee, H.; Lee, K.; Kim, I.-K.; Park, T. G. *Adv. Funct. Mater.* **2009**, *19*, 1884-1890.

(14) Li, C.; Shi, G. *J. Photochem. Photobiol. C* **2014**, *19*, 20-34.

(15) Liu, R.; Chen, Z.; Wang, Y.; Cui, Y.; Zhu, H.; Huang, P.; Li, W.; Zhao, Y.; Tao, Y.; Gao, X. *Acs Nano* **2011**, *5*, 5560-5565.

(16) Lu, C.-H.; Yang, H.-H.; Zhu, C.-L.; Chen, X.; Chen, G.-N. *Angew. Chem. Int. Ed.* **2009**, *48*, 4785-4787.

(17) He, S.; Song, B.; Li, D.; Zhu, C.; Qi, W.; Wen, Y.; Wang, L.; Song, S.; Fang, H.; Fan, C. *Adv. Funct. Mater.* **2010**, *20*, 453-459.

(18) Peng, C.; Hu, W.; Zhou, Y.; Fan, C.; Huang, Q. *Small* **2010**, *6*, 1686-1692.

(19) Ge, J.; Ou, E.-C.; Yu, R.-Q.; Chu, X. *J. Mater. Chem. B* **2014**, *2*, 625-628.

(20) Huang, Y.; Shi, Y.; Yang, H. Y.; Ai, Y. *Nanoscale* **2015**, *7*, 2245-2249.

(21) Zhu, C.; Zeng, Z.; Li, H.; Li, F.; Fan, C.; Zhang, H. *J. Am. Chem. Soc.* **2013**, *135*, 5998-6001.

(22) Li, J.; Huang, Y.; Wang, D.; Song, B.; Li, Z.; Song, S.; Wang, L.; Jiang, B.; Zhao, X.; Yan, J.; Liu, R.; He, D.; Fan, C. *Chem. Commun.* **2013**, *49*, 3125-3127.

(23) Wu, M.; Kempaiah, R.; Huang, P.-J. J.; Maheshwari, V.; Liu, J. *Langmuir* **2011**, *27*, 2731-2738.

(24) Hummers, W.; Offeman, R. *J. Am. Chem. Soc.* **1958**, *80, 1339-1339*.

For TOC only